Journal of Electroanalytical Chemistry 880 (2021) 114928

Contents lists available at ScienceDirect

Journal of Electroanalytical Chemistry

journal homepage: www.elsevier.com/locate/jelechem

Short communication

Short communication: Molecular architecture based on palladium-salen complex/graphene for low potential water oxidation

Yuri A. Oliveira, André Olean-Oliveira, Marcos F.S. Teixeira *

Department of Chemistry and Biochemistry, School of Science and Technology - Sao Paulo State University (UNESP), Rua Roberto Simonsen 305, Presidente Prudente, SP 19060-900, Brazil

ARTICLE INFO

Article history:
Received 19 August 2020
Received in revised form 3 December 2020
Accepted 7 December 2020
Available online 10 December 2020

Keywords:
Electrocatalysis
Water splitting
Metallopolymer
Electrochemical impedance
Water oxidation

ABSTRACT

We have developed electrocatalytic platforms based on palladium metallopolymer-graphene for the water splitting reaction. The platforms presented a low potential for the water oxidation reaction. By cyclic voltammetry and electrochemical impedance spectroscopy (EIS), the interfacial phenomena were investigated, allowing us to obtain important results that helped to determine kinetic and mechanistic information. The studies revealed that the introduction of graphene in the metallopolymer matrix increased the turnover frequency (TOF) value. Analysis of the Tafel plots obtained from the EIS data also revealed a change in the reaction mechanism after the introduction of graphene. The new platform demonstrated its applicability in the water splitting reaction for use in fuel cells.

1. Introduction

The current lifestyle in addition to the increased world population has led to increasing energy demands [1]. The racing for the development of new and alternative energy sources aims to replace fossil fuel sources as well as to develop more effective technologies to meet the great energy demand that will come in the coming decades [2]. Fuel cells based on hydrogen production and combustion are among the main sustainable sources of energy, which are able to generate energy through electrochemical reactions and decrease the environmental impact.

The oxygen evolution reaction (OER) is an important and limiting half-reaction in the electrochemical water splitting process due to the slow kinetics of the reaction and high energetic barrier [3]. Therefore, the development of new electrocatalytic materials with the objective of reducing the energy barrier as well as increasing the kinetic efficiency of the OER has been extensively investigated [4–8].

The use of catalyst materials based on metal complexes for the OER has been studied, with promising results [7]. Therefore, the present work has the goal of investigating two different palladium Schiff base architectures for the OER. The investigations were based mainly on the electrochemical impedance spectroscopy (EIS) technique. The results are promising and can contribute greatly to the discussion and understanding of similar electrochemical systems.

2. Results and discussion

The use of materials based on palladium complexes for electrocatalytic reactions has been investigated for several purposes [9–12]. In the case of the water oxidation reaction, the main advantage of such complexes is the good electrocatalytic performance in an acid medium [13]. The present work proposes the investigation of two platforms with different architectures based on the palladium Schiff base complex (Fig. 1A), aiming to decrease the onset potential values for the oxygen evolution reaction. Electrocatalytic platforms were easily obtained using the electropolymerization technique, which allowed great control over the electrodeposited materials [14–16].

Films of metal-salen complexes have shown electrocatalytic activity for a number of electrooxidation reactions. In addition, the spatial arrangement in the form of molecular columns allows us to obtain a large contact surface, increasing the catalytic activity [15–18]. Additionally, it is known that the incorporation of graphene into the metallopolymer matrix tends to increase the electrocatalytic performance of materials [19]. Therefore, palladium metallopolymer (poly[Pd(salen)], Fig. 1A) and palladium metallopolymer-graphene (poly[Pd(salen)]-G, Fig. 1B) films were built to investigate their catalytic properties for application in the OER. SEM images of the different electrocatalytic platforms demonstrate a complete covering and uniform distribution of electrocatalytic materials on the FTO surface with both architectures (Fig. 1C–F). In the poly[Pd(salen)] electrode, nanostructures with alveolar shapes were found (**Fig. 1F** and **D**),

* Corresponding author.
E-mail address: marcos.fs.teixeira@unesp.br (M.F.S. Teixeira).

http://dx.doi.org/10.1016/j.jelechem.2020.114928

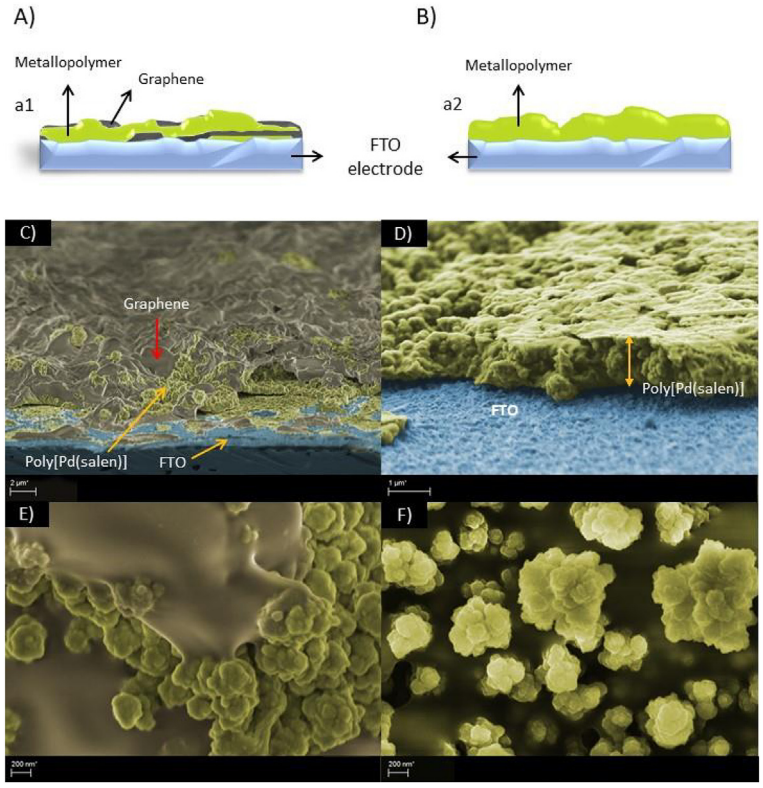

Fig. 1. A–B) Schematic representation of electrocatalytic platform design. SEM cross-sectional (**Fig. C** and **Fig. D**) and superficial images (**Fig. E** and **Fig. F**) of poly[Pd(salen)]-graphene and poly[Pd(salen)] on the FTO electrode surface.

characteristic of films based on metal salen [14,20,21]. The poly[Pd(salen)]-G film demonstrated a surface covering similar to that of the film containing only the metallopolymer, demonstrating that the poly[Pd(salen)] film could also be grown on a graphene surface. However, the cross-sectional images also showed layers of graphene inside the film (see Fig. 1C). The results demonstrated the effectiveness of the layered alternate strategy.

The electrocatalytic activity of the different platforms built for OER was investigated in 0.10 mol L^{-1} H_2SO_4 solution at 25 mV s^{-1} (Fig. 2) using a three-electrode configuration. It is known that the thermodynamic potential for water oxidation is 1.23 V (vs. RHE) (SCE = 0.989 V) [7,22]. Under the same conditions mentioned above, the onset values of +0.80 V and +0.62 V vs. RHE (pH 1) were found for the poly[Pd(salen)] and poly[Pd(salen)]-G electrocatalytic platforms, respectively. The onset potential for water oxidation on platinum electrode was +1.10 V vs. RHE (pH 1). Comparatively, the catalytic current of the poly[Pd(salen)]-G and poly[Pd(salen)] electrodes was 37-times and 12-times high than to the platinum electrode at isopotentials of +080 V and +1.0 vs. SCE, respectively. No redox process was observed at the unmodified FTO platform as a working electrode (curve d).

The electrocatalytic activities of the poly[Pd(salen)] and poly[Pd(salen)]-G electrodes were also investigated using the electrochemical impedance spectroscopy (EIS) technique. EIS is a powerful tool for analyzing interfacial phenomena [23]. The spectra were obtained for the two different platforms at an applied potential of +0.50 V vs. SCE (Fig. 3A). The potential chosen was based on data obtained by voltammetry; this was found after onset potential for both platforms. However, at this point, a significant current value was recorded for the poly[Pd(salen)]-G platform, but for the poly[Pd(salen)] platform, the value was 8 times lower. EIS allowed an accurate analysis of the electrochemical phenomena, providing important information on the OER with the electrocatalytic platforms. Analysis of the obtained spectra was performed based on the equivalent circuit models (ECMs) shown in

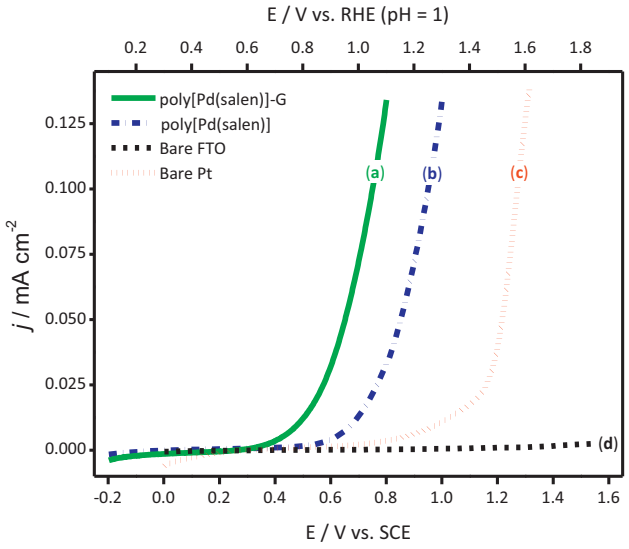

Fig. 2. Voltammetric response to poly[Pd(salen)]-G (curve **a** – olive line); poly[Pd(salen)] (curve **b** – blue shirt dash dot); bare Pt (curve **c** – red short dot) and bare FTO (curve **d** – black short dash) in 0.10 mol L^{-1} H_2SO_4 (pH 1.0) solution under a N_2 atm. Scan rate = 25 mV s^{-1}.

Fig. 3C–D. The values obtained from the mathematical adjustments are summarized in Table 1.

The proposed ECMs were based on previous work on thin films of metallopolymers and on the basis of the analysis of the BODE spectra (Fig. 3B), where two frequency peaks were visible [15,16]. The ECMs for the different platforms showed similarities; however, they showed some modifications due to the different molecular arrangements of the

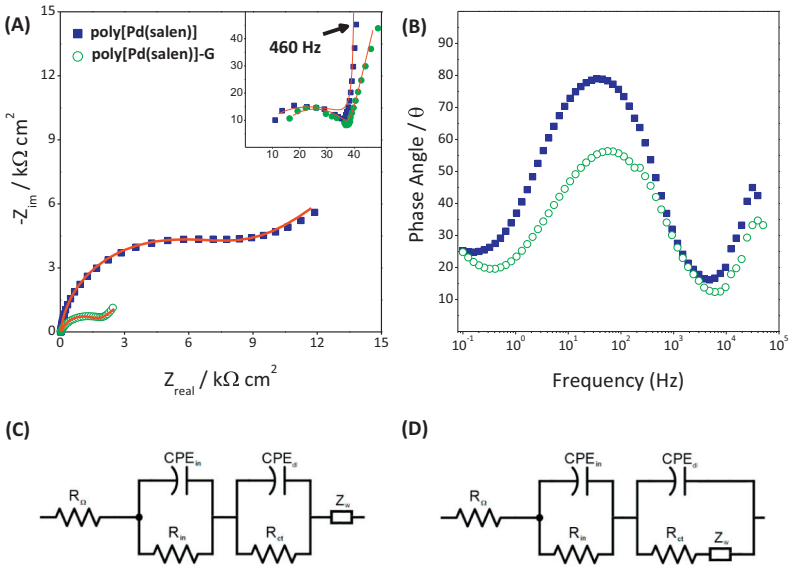

Fig. 3. Nyquist (**A**) and BODE (**B**) plots for the electrocatalytic platforms in 0.1 mol L^{-1} H_2SO_4 (pH 1.0) at +0.50 V vs. SCE (+0.80 V vs. RHE). ECMs for poly[Pd(salen)]-G (**C**) and poly[Pd(salen)] (**D**).

Table 1
Physicochemical parameters determined from fitting of the electrochemical impedance spectra of the poly[Pd(salen)] and poly[Pd(salen)-G films using the ECMs shown in Fig. 3D and Fig. 3C, respectively. R_Ω = 10 Ω cm^2. The fitting error was ≤2%.

Catalytic platform	R_{in} (kΩ cm^2)	R_{ct}	CPE_{in} μF cm^{-2} $s^{\alpha-1}$	α_{in}	CPE_{dl} μF cm^{-2} $s^{\alpha-1}$	α_{dl}	Z_W kΩ $s^{-0.5}$ cm^2	ECMs
[Pd(salen)]	0.030	7.64	0.33	0.99	10.9	0.95	4.00	Fig. 3D
[Pd(salen)]-G	0.029	1.48	0.21	0.99	41.7	0.83	0.81	Fig. 3C

electrocatalytic films. The first term of the ECM, in the high-frequency range (50 to 10 kHz), was common for all platforms showing a solution resistance (R_Ω) in series with a parallel combination of the resistance associated with the film/electrode interface (R_{in}) and the geometric capacitance of the system (CPE_{in}). There was no significant R_{in} differentiation between the films, with the values being virtually equivalent. This result is because the material in contact with the FTO electrode was Pd(salen) in both electrocatalytic platforms. For the second term of the ECMs, in the medium-low frequency region (10 kHz to 0.10 Hz), both platforms presented a charge transfer resistance (R_{ct}) associated with redox processes occurring at the electrode/solution interface and a capacitance associated with a double electrical layer (CPE_{dl}).

The faradaic resistance here is attributed to the sum of the resistances involved in the OER stages; therefore, it should be interpreted as being the resistance equivalent to the sum of the resistances involved in the water oxidation reaction [24]. Therefore, there was a significant decrease in the R_{ct} value for the architecture containing graphene in the metallopolymeric matrix. This value was approximately 5 times lower than that for the platform containing only poly[Pd(salen)]. The decrease in the R_{ct} value for the poly[Pd(salen)]-G film can be interpreted as an increase in the catalytic performance since its value is associated with the kinetic steps of the OER [25,26]. The gain in electrocatalytic performance can be related to the synergistic effect from the incorporation of graphene sheets into the poly[Pd(salen)] film. The increase in performance was also related to an increased surface area for the platform containing graphene, which was verified among the CPE_{dl} values [25].

However, the models differed in the position of the sixth element. For the poly[Pd(salen)] film, the element for the diffusion of species according to the catalysis of water molecules, a Warburg element (W), was presented in series with the R_{ct} (Fig. 3D). This model is suitable for simple faradaic reactions limited by the diffusion mechanism [27,28]. In the case of the poly [Pd(salen)]-G film, the Warburg element is in series with the second term of the ECM (Fig. 3C). This difference in the arrangement of the elements reveals changes in the electrocatalytic mechanisms of the OER [29]. The model containing the Warburg element in series with the parallel combination is associated with complex reactions involving adsorbed species and diffusion of more than one species [29]. The Warburg element may be associated with the diffusion of the anion during the electrochemical oxidation of palladium and with the O_2 generated in the oxidation of water. Thus, for the poly[Pd(salen)] film, the applied potential of +0.50 V vs. SCE is sufficient to promote the oxidation of catalytic sites (metallic centers from Pd^{II} to Pd^{III}), but this potential is not enough to promote the oxidation reaction of water. On the other hand, the poly[Pd(salen)]-G film at the same potential is capable of promoting the water oxidation reaction. Such data reveal that the alternating architecture results in a decrease in the potential required for the OER.

To compare the electrocatalytic performance of the developed platforms, the turnover frequency (TOF) values were calculated through the following relation (Eq. (1)) [30]:

$$TOF = \frac{j}{nF\Gamma} \quad (1)$$

where j is the current density at a given potential (A cm^{-2}), n is the number of electrons involved in the reaction (OER = $4e^-$), F is the Faraday constant (96,485 A s mol^{-1}) and Γ is the surface-active site concentration (mol cm^{-2}). The Γ values were calculated based on the Γ = Q/nFA relationship, where Q is charge, which was obtained from the apparent capacitance values (C_{app}) calculated from the CPE_{dl} values by Eq. (2) [31,32].

$$C_{app} = \frac{(R_{ct}CPE_{dl})^{1/\alpha}}{R_{ct}} \quad (2)$$

Table 2
Performance of different OER catalytic materials.

Electrode	TOF (s^{-1})	Onset (V vs. RHE)	Ref.
$Pd(acac)_2$	0.2	1.43	[25]
NiFe-SW	8.7	1.45	[33]
PdP_2@CB	0.32	1.59	[34]
Co-Pi/W:$BiVO_4$	–	0.77	[35]
$CuWO_4$	–	0.58	[36]
Pd(salen)	0.07	0.80	Present work
Pd(salen)-G	0.25	0.62	

The TOF values reveal the rate of regeneration of the catalytic sites after the catalytic reaction [30]. TOF values of 0.25 and 0.07 s^{-1} were verified for the poly[Pd(salen)]-G and poly[Pd(salen)] films, respectively. The values demonstrate that the film containing graphene exhibits the best electrocatalytic performance. Furthermore, the values obtained were comparable to those of OER electrodes found in the literature (Table 2).

Tafel curves were obtained using data obtained by EIS (Fig. 4). Previous studies point out the advantage of the EIS method because its data are obtained in the steady state and because it does not influence the resistance of the solution (R_Ω), disassociate the capacitive elements (film and double layer capacitance) of the system or interfere with the accuracy of the results [2,24]. Through the obtained slope values and assuming that the charge transfer coefficient (ctc) value is equal to ~0.5, it was verified that the electrode containing alternating graphene layers has $2e^-$ being transferred in the reaction-determining step (rds) against $1e^-$ of the electrode containing only the metallopolymer film. The result suggests a change in the OER mechanism between electrodes containing graphene and those without graphene.

Based on the above data, the mechanism for the poly[Pd(salen)]-G electrode is possibly similar to the electrochemical path model (Eqs. (3)–(5)) [2]:

$$\text{poly}\left[\text{Pd}^{\text{II}}(\text{salen})\right] + \text{H}_2\text{O} \rightarrow \text{poly}\left[\text{Pd}^{\text{III}}(\text{salen})\right]\text{OH} + \text{e}^- + \text{H}^+ \quad (3)$$

$$2\,\text{poly}\left[\text{Pd}^{\text{III}}(\text{salen})\right]\text{OH} \rightarrow \text{poly}\left[\text{Pd}^{\text{III}}(\text{salen})\right]-\text{O}_2-\text{poly}\left[\text{Pd}^{\text{III}}(\text{salen})\right] + 2\text{e}^- + 2\text{H}^+ \text{ r.d.s} \quad (4)$$

$$\text{poly}\left[\text{Pd}^{\text{III}}(\text{salen})\right]-\text{O}_2-\text{poly}\left[\text{Pd}^{\text{III}}(\text{salen})\right] \rightarrow 2\,\text{poly}\left[\text{Pd}^{\text{II}}(\text{salen})\right] + \text{O}_2 \quad (5)$$

The stability analysis of the poly[Pd(salen)]-G was obtained by chronoamperometry under constant anodic polarization (+0.80 vs SCE) in 0.10 mol L^{-1} H_2SO_4 solution (pH 1.0 Only a slight decrease of 11% in the current was observed after 2 h of electrolysis with a current density limit of 0.11 mA cm^2.

3. Conclusion

Electrodes modified with palladium metallopolymer and palladium metallopolymer-graphene showed good onset potential values for the OER. In addition, it was possible to investigate the physicochemical properties of the interface by EIS and demonstrate that the poly[Pd(salen)]-G film performed OER at low overpotential, whereas the poly[Pd(salen)] film was still in the initial stage of the reaction. The alternating architecture film showed the best performance based on the TOF and Tafel calculations, which can be related to the presence of graphene in the polymeric matrix and the increased surface area, as observed in the SEM images. This electrocatalytic material can be adapted for use in electrochemical reactors for water splitting. Efforts are being made to fully elucidate the mechanisms responsible for the oxidation of water in potentials below the expected for the thermodynamic potential.

4. Experimental

The ligand 2,2′-{1,2-ethanediylbis[nitrilo(*E*)methylylidene]} diphenolate (salen) was purchased from Sigma-Aldrich and used without further purification. The catalytic complex Pd(II) 2,2′-{1,2-ethanediylbis [nitrilo(*E*)methylylidene]}diphenolate (Pd(salen)) was obtained by the addition of stoichiometric and equimolar (5.0 mmol) amounts of the salen ligand and palladium acetate (Sigma-Aldrich) in absolute ethanol (50 mL). The solution was kept under reflux for 3 h at 50 °C with constant stirring to yield a yellow precipitate. The precipitate was filtered in a Gooch crucible, washed with absolute ethanol and kept in a desiccator. FTIR (ν cm-1) in KBr: 3339, –OH_{ph}; 1612, C=N; 1505, C=C; 1291, >C–O_{ph}; 1023, ring

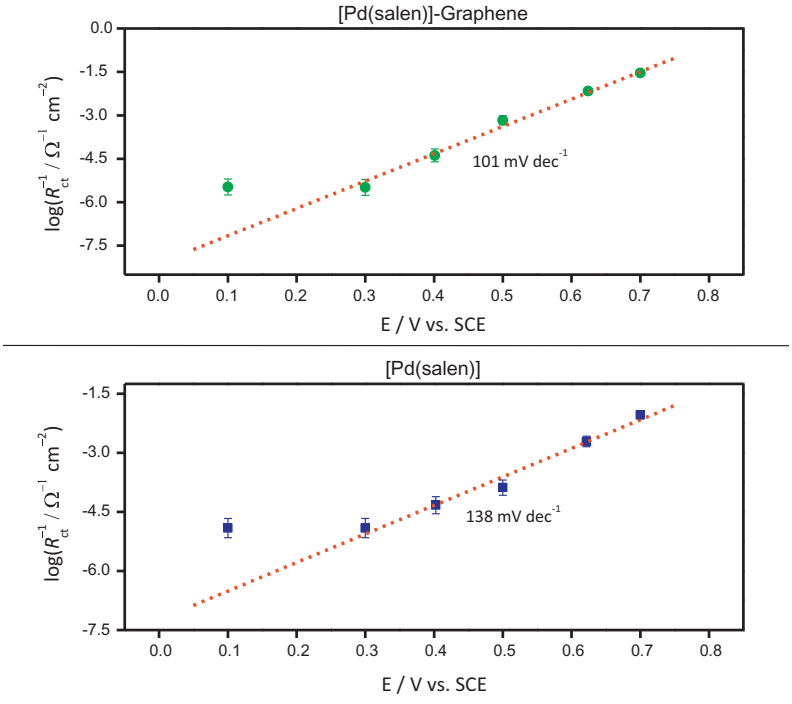

Fig. 4. Dependence of reciprocal R_{ct} on the potential for OER on Pd(salen)-electrocatalytic platforms in 0.10 mol L^{-1} H_2SO_4. $n = 3$.

breathing; and 501, PdO. UV–vis (nm) in CH_3CN: 250 ($\pi \rightarrow \pi^*$); 326 ($\pi \rightarrow \pi^*$); 403 ($n \rightarrow \pi^*$); and 547 (MLCT).

The coating of fluorine-doped tin oxide (FTO) electrode surfaces (geometric area = 1.0 cm^2) with poly[Pd(salen)] and poly[Pd(salen)]-graphene catalytic films was performed in a conventional electrochemical cell with three electrodes, including a saturated calomel electrode (SCE) ($E_{RHE} = E_{SCE} + 0.241 + 0.0591pH$) as the reference electrode and a platinum wire electrode as the auxiliary electrode. Measurement management was performed by a μ-Autolab type III potentiostat/galvanostat (Eco Chimie). The polymer [Pd(salen)] film was formed by electropolymerization using 1.0 mmol L^{-1} Pd(salen) complex in acetonitrile with 0.10 mol L^{-1} tetrabutylammonium hexafluorophosphate (HFTBA) electrolyte while applying 10 scan cycles in a potential range of 0.0 to 1.4 V vs. SCE at 100 mV s^{-1} in a N_2 atmosphere. In contrast, poly[Pd(salen)]-graphene was manufactured by applying 10 alternate layers of metallopolymer and graphene. This process was performed by applying an electropolymerization cycle of the monomer [Pd(salen)], as described above, and then exchanging the solution with a solution containing 1.0 mg mL^{-1} graphene suspension in acetonitrile/HFTBA and applying one scan cycle in the potential range of 0.0 to −0.50 V at a scan rate of 100 mV s^{-1}. These steps were repeated 9 more times.

The EIS measurements were performed through the incidence of a sine wave of 10 mV applied in a frequency range of 50 kHz to 0.1 Hz with 10 steps dec^{-1}. All spectra were recorded at 25 °C. Analysis of the complex plane impedance spectra was performed by ZPlot 2.4 software. The cross-sectional scanning electron microscopy (SEM) image was performed by cleaving an FTO electrode containing the metallopolymer using a cut on its non-conductive side by a diamond-tipped pen.

Supplementary data to this article can be found online at https://doi.org/10.1016/j.jelechem.2020.114928.

Declaration of Competing Interest

The authors declare that they have no known competing financial interests or personal relationships that could have appeared to influence the work reported in this paper.

Acknowledgement

The authors acknowledge FAPESP (2016/09017-1); CEPID-FAPESP (2013/07296-2) and CNPq (301298/2017-3) for their financial support. A.O.O. thanks CAPES (88882.434480/2019-01) for PhD fellowship. SJT and NSA.

References

[1] I.B. Pehlivan, M.A. Arvizu, Z. Qiu, G.A. Niklasson, T. Edvinsson, Impedance spectroscopy modeling of nickel-molybdenum alloys on porous and flat substrates for applications in water splitting, J. Phys. Chem. C 123 (2019) 23890–23897.
[2] S. Anantharaj, S.R. Ede, K. Karthick, S.S. Sankar, K. Sangeetha, P.E. Karthik, S. Kundu, Precision and correctness in the evaluation of electrocatalytic water splitting: revisiting activity parameters with a critical assessment, Energy Environ. Sci. 11 (2018) 744–771.
[3] V.S. Kalimuthu, R. Attias, Y. Tsur, Electrochemical impedance spectra of RuO2 during oxygen evolution reaction studied by the distribution function of relaxation times, Electrochem. Commun. 110 (2020) Article 106641.
[4] H. Feizi, F. Shiri, R. Bagheri, J.P. Singh, K.H. Chae, Z.L. Song, M.M. Najafpour, The application of a nickel(II) Schiff base complex in water oxidation: the importance of nanosized materials, Catal. Sci. Technol. 8 (2018) 3954–3968.
[5] C.J. Wang, Y. Chen, W.F. Fu, New platinum and ruthenium Schiff base complexes for water splitting reactions, Dalton T 44 (2015) 14483–14493.
[6] H.Y. Chen, Z.J. Sun, X. Liu, A. Han, P.W. Du, Cobalt-Salen complexes as catalyst precursors for Electrocatalytic water oxidation at low Overpotential, J. Phys. Chem. C 119 (2015) 8998–9004.
[7] J.D. Blakemore, R.H. Crabtree, G.W. Brudvig, Molecular catalysts for water oxidation, Chem. Rev. 115 (2015) 12974–13005.
[8] C. Wei, R.R. Rao, J.Y. Peng, B.T. Huang, I.E.L. Stephens, M. Risch, Z.C.J. Xu, Y. Shao-Horn, Recommended practices and benchmark activity for hydrogen and oxygen electrocatalysis in water splitting and fuel cells, Adv. Mater. 31 (2019).
[9] N.U. Babar, K.S. Joya, M.A. Ehsan, M. Khan, M. Sharif, Noble-metal-free colloidal-copper based low overpotential water oxidation electrocatalyst, Chemcatchem 11 (2019) 6022–6030.
[10] S. Sarkar, S.C. Peter, An overview on Pd-based electrocatalysts for the hydrogen evolution reaction, Inorg. Chem. Front. 5 (2018) 2060–2080.
[11] G.A. El-Nagar, A.F. Darweesh, I. Sadiek, A novel nano-palladium complex anode for formic acid electro-oxidation, Electrochim. Acta 215 (2016) 334–338.
[12] S. Chatterjee, C. Griego, J.L. Hart, Y.W. Li, M.L. Taheri, J. Keith, J.D. Snyder, Free standing nanoporous palladium alloys as CO poisoning tolerant electrocatalysts for the electrochemical reduction of CO2 to formate, ACS Catal. 9 (2019) 5290–5301.
[13] B.M. Hunter, H.B. Gray, A.M. Muller, Earth-abundant heterogeneous water oxidation catalysts, Chem. Rev. 116 (2016) 14120–14136.
[14] C.R. Peverari, D.N. David-Parra, M.M. Barsan, M.F.S. Teixeira, Mechanistic study of the formation of multiblock pi-conjugated metallopolymer, Polyhedron 117 (2016) 415–421.
[15] C.F. Pereira, A. Olean-Oliveira, D.N. David-Parra, M.F.S. Teixeira, A chemiresistor sensor based on a cobalt(salen) metallopolymer for dissolved molecular oxygen, Talanta 190 (2018) 119–125.
[16] A. Olean-Oliveira, C.F. Pereira, D.N. David-Parra, M.F.S. Teixeira, Electrocatalytic study of the thin metallopolymer film of [2,2 '-{1,2-Ethanediylbis[Nitrilo(1E)-1-Ethyl-1-Ylidene]} Diphenolate]-nickel(II) for ethanol Electrooxidation, Chemelectrochem 5 (2018) 3557–3565.
[17] M. Vilas-Boas, C. Freire, B. de Castro, A.R. Hillman, Electrochemical characterization of a novel salen-type modified electrode, J. Phys. Chem. B 102 (1998) 8533–8540.
[18] M. Vilas-Boas, C. Freire, B. de Castro, P.A. Christensen, A.R. Hillman, Spectroelectrochemical characterisation of poly[Ni(saltMe)]-modified electrodes, Chem-Eur. J. 7 (2001) 139–150.
[19] M.F. Zhang, Y. Li, Z.Q. Su, G. Wei, Recent advances in the synthesis and applications of graphene-polymer nanocomposites, Polym. Chem-Uk. 6 (2015) 6107–6124.
[20] Y.K. Zhang, J.L. Li, F. Gao, F.Y. Kang, X.D. Wang, F. Ye, J. Yang, Electropolymerization and electrochemical performance of salen-type redox polymer on different carbon supports for supercapacitors, Electrochim. Acta 76 (2012) 1–7.
[21] A.A. Vereschagin, V.V. Sizov, P.S. Vlasov, E.V. Alekseeva, A.S. Konev, O.V. Levin, Water-stable [Ni(salen)]-type electrode material based on phenylazosubstituted salicylic aldehyde imine ligand, New J. Chem. 41 (2017) 13918–13928.
[22] J.E. Yourey, K.J. Pyper, J.B. Kurtz, B.M. Bartlett, Chemical stability of CuWO4 for Photoelectrochemical water oxidation, J. Phys. Chem. C 117 (2013) 8708–8718.
[23] J.B. Jorcin, M.E. Orazem, N. Pebere, B. Tribollet, CPE analysis by local electrochemical impedance spectroscopy, Electrochim. Acta 51 (2006) 1473–1479.
[24] R.L. Doyle, M.E.G. Lyons, An electrochemical impedance study of the oxygen evolution reaction at hydrous iron oxide in base, Phys. Chem. Chem. Phys. 15 (2013) 5224–5237.
[25] K.S. Joya, M.A. Ehsan, N.U.A. Babar, M. Sohail, Z.H. Yamani, Nanoscale palladium as a new benchmark electrocatalyst for water oxidation at low overpotential, J. Mater. Chem. A 7 (2019) 9137–9144.
[26] M.G. Gao, L. Yang, B. Dai, X.H. Guo, Z.Y. Liu, B.H. Peng, A novel Ni-Schiff base complex derived electrocatalyst for oxygen evolution reaction, J. Solid State Electrochem. 20 (2016) 2737–2747.
[27] M. Oldenburger, B. Bedurftig, A. Gruhle, F. Grimsmann, E. Richter, R. Findeisen, A. Hintennach, Investigation of the low frequency Warburg impedance of Li-ion cells by frequency domain measurements, J. Energy Storage. 21 (2019) 272–280.
[28] M.D. Levi, Z. Lu, D. Aurbach, Application of finite-diffusion models for the interpretation of chronoamperometric and electrochemical impedance responses of thin lithium insertion V2O5 electrodes, Solid State Ionics 143 (2001) 309–318.
[29] A. Lasia, Electrochemical Impedance Spectroscopy and its Applications, Springer-Verlag, New York, 2014.
[30] M. Nakayama, Y. Fujii, K. Fujimoto, M. Yoshimoto, A. Kaide, T. Saeki, H. Asada, Electrochemical synthesis of a nanohybrid film consisting of stacked graphene sheets and manganese oxide as oxygen evolution reaction catalyst, RSC Adv. 6 (2016) 23377–23382.
[31] C.L. Alexander, B. Tribollet, M.E. Orazema, Influence of micrometric-scale electrode heterogeneity on electrochemical impedance spectroscopy, Electrochim. Acta 201 (2016) 374–379.
[32] M. de Pauli, A.M.C. Gomes, R.L. Cavalcante, R.B. Serpa, C.P.S. Reis, F.T. Reis, M.L. Sartorelli, Capacitance spectra extracted from EIS by a model-free generalized phase element analysis, Electrochim. Acta 320 (2019) Article 134366.
[33] W. Zhang, Y.Z. Wu, J. Qi, M.X. Chen, R. Cao, A thin nife hydroxide film formed by stepwise electrodeposition strategy with significantly improved catalytic water oxidation efficiency, Adv. Energy Mater. 7 (2017) Article 1602547.
[34] F. Luo, Q. Zhang, X.X. Yu, S.L. Xiao, Y. Ling, H. Hu, L. Guo, Z.H. Yang, L. Huang, W.W. Cai, H.S. Cheng, Palladium phosphide as a stable and efficient Electrocatalyst for overall water splitting, Angew. Chem. Int. Edit. 57 (2018) 14862–14867.
[35] D.K. Zhong, S. Choi, D.R. Gamelin, Near-complete suppression of surface recombination in solar Photoelectrolysis by "co-pi" catalyst-modified W:BiVO4, J. Am. Chem. Soc. 133 (2011) 18370–18377.
[36] J.E. Yourey, B.M. Bartlett, Electrochemical deposition and photoelectrochemistry of CuWO4, a promising photoanode for water oxidation, J. Mater. Chem. 21 (2011) 7651–7660.